# Accepted Manuscript

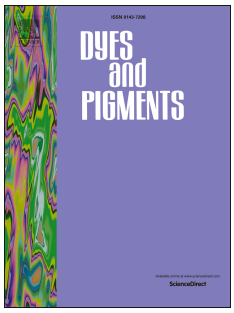


A colorimetric and turn-on fluorescent chemosensor for selectively sensing $Hg^{2+}$ and its resultant complex for fast detection of $I^{-}$ over $S^{2-}$

Ximing Huang, Zhengliang Lu, Zhuo Wang, Chunhua Fan, Wenlong Fan, Xiaomin Shi, Haitao Zhang, Meishan Pei

PII: S0143-7208(16)00011-5

DOI: 10.1016/j.dyepig.2016.01.008

Reference: DYPI 5061

To appear in: *Dyes and Pigments*

Received Date: 27 October 2015

Revised Date: 5 January 2016

Accepted Date: 6 January 2016

Please cite this article as: Huang X, Lu Z, Wang Z, Fan C, Fan W, Shi X, Zhang H, Pei M, A colorimetric and turn-on fluorescent chemosensor for selectively sensing $Hg^{2+}$ and its resultant complex for fast detection of $I^{-}$ over $S^{2-}$, *Dyes and Pigments* (2016), doi: 10.1016/j.dyepig.2016.01.008.

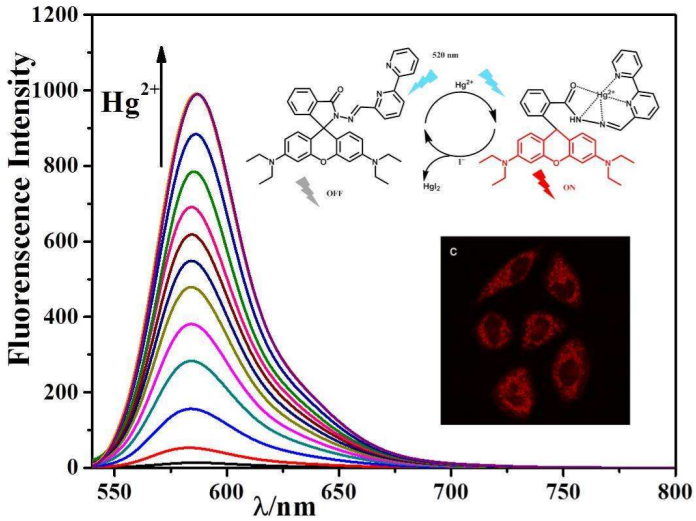

# A colorimetric and turn-on fluorescent chemosensor for selectively sensing $Hg^{2+}$ and its resultant complex for fast detection of $I^-$ over $S^{2-}$

Ximing Huang,[†] Zhengliang Lu,*,[†] Zhuo Wang,[‡] Chunhua Fan,[†] Wenlong Fan,[†] Xiaomin Shi[†], Haitao Zhang,[†] Meishan Pei[†]

[†]*Key Laboratory of Chemical Sensing & Analysis in Universities of Shandong (University of Jinan), School of Chemistry and Chemical Engineering, University of Jinan, Jinan 250022, China*

[‡] *Faculty of Science, Beijing University of Chemical Technology, Beijing, 100029, China.*

## Abstract

A novel bipyridine-functionalized turn-on fluorescent chemosensor was successfully synthesized and fully characterized by $^1$H NMR, $^{13}$C NMR and MS, UV-Vis and fluorescence spectroscopies. The sensor specifically binds to $Hg^{2+}$ over other competing ions with a significant fluorescence enhancement as well as a visual colour change under physiological conditions. The detection limit of $Hg^{2+}$ was as low as 32 nM, confirming very high sensitivity toward $Hg^{2+}$. Moreover, the fluorescence intensity and colour change of the sensor-$Hg^{2+}$ was quenched by $I^-$ or $S^{2-}$ and was proportional to their concentrations with a detection limit of 0.37 μM and 0.43 μM, respectively. The reaction of $I^-$ grabbing $Hg^{2+}$ from the sensor-$Hg^{2+}$ finished in 10 seconds due to a stronger binding force, much faster than that of $S^{2-}$, which allowed fast detection of $I^-$ over $S^{2-}$ even in a competent environment. In addition, the sensor was successfully used for the highly sensitive detection of $Hg^{2+}$ in living cells.

**Keywords: colorimetric, chemosensor, mercury, iodide, sulphide**

## 1. Introduction

The developments of multifunctional chemosensors for heavy and transition metal cations as well as various anions have attracted considerable attention due to their potential applications in biological and environmental systems [1-4]. As one of the most toxic metals mercury (Hg) can significantly destroy human central nervous system and endocrine system [5-7]. Even a very low level of $Hg^{2+}$ can disturb a series of cellular processes and consequently trigger serious health disorders in the human body, such as Minamata, edema and anemia [8-11]. Moreover, mercury ion ($Hg^{2+}$) from artificial and mineral processes such as gold mining, fossil fuel combustion, and chemical manufacturing can be released into the natural environment, accumulated in food chains, and finally entered into higher trophic biological systems [12]. The World Health Organization (WHO) has strictly stipulated that the level of $Hg^{2+}$ is not more than 0.001 $mg \cdot L^{-1}$ in drinking water [13]. Among various chemically and biologically important anions, $I^-$ is one of dispensable elements in human body and the heaviest element commonly needed by living organisms [14-16]. Iodide deficiency leads to mental retardation and thyroid gland dysfunction and increases the risk of breast and stomach cancer [17]. Release of excessive $I^-$ ions and iodine can damage environment and physical systems.[18]Also $H_2S$ from industrial processes such as sewage plants and petroleum refining results in serious environmental pollution. Moreover, endogenic sulfide ions from microbial reduction of sulfate and sulfur-containing amino acids can destroy mucous membranes and brain tissues, which are correlated with Alzheimer's disease, Down's syndrome, and diabetes

[19-24]. So it is urgent to develop novel analytical methods with high sensitivity and selectivity to detect $I^-$ and $S^{2-}$ ions as well as $Hg^{2+}$ in either aqueous or non-aqueous media.

Fluorescence methodology has been widely used as a great tool for detection of metal ions and anions due to its operational simplicity, high sensitivity and selectivity, and ease of observation over traditional methods such as inductively coupled plasma mass spectrometry, atomic absorption, and chemiluminescence [25-28]. Thus, numerous colorimetric and fluorescent chemosensors have been reported in the recent literatures for selective and sensitive sensing of $Hg^{2+}$ [29-35], $I^-$ [36-38] and $S^{2-}$ [39-41] ions, respectively. As a matter of fact, few multifunctional probes sensing metal ions and anions have been reported [42, 43]. Without doubt, it is of challenge to rationally design simple, practical multifunctional chemosensors in aqueous media.

Usually, the construction of fluorescent sensors depends on rational combinations of recognition sites and signalling subunits [44]. It is well known that each signalling subunit has its own distinct emission spectrum and each recognition group could detect a wide array of ions. Even the subtle changes of the linker such as incorporation of either a single- or double-bond could dramatically influence the detection efficiency of designed probes. For example, Duan's group reported the probe **P1** constructed through the condensation of rhodamine 6G hydrazide and 2-pyridinecarboxaldehyde (Scheme 1a), which can detect $Hg^{2+}$ in 1:1 (v/v) $H_2O$/DMF solution with very high efficiency [45]. Later, Zhang's group reported that the probe **P2** (Scheme 1b), obtained through reducing probe **P1**, could rapidly sense $Cu^{2+}$ within

one minute in buffered $H_2O$/EtOH (8:2, v/v, Tris-HCl, pH 7.1) [46]. Probe **P3** containing thiophene tailed pyridine as the recognition group could detect $Zr^{4+}$ in $CH_3OH$-$H_2O$ (4:1, 1/1, HEPES, 10 μM, pH 7.4) (Scheme 1c) [47]. Furthermore, ligand-metal ensembles tend to selectively and sensitively recognize anions in aqueous solutions [48-52].

Encouraged by these excellent studies and speculations, a multifunctional chemosensor **RBP** (Scheme 2) was constructed based on the rhodamine fluorescence platform combining a 2,2`-bipyridyl recognition site. As anticipated, the binding of **RBP** with $Hg^{2+}$ triggered the opening of the spirolactam ring of the rhodamine moiety in neutral aqueous solutions with remarkably high sensitivity and selectivity. Interestingly, the ensemble **RBP**-$Hg^{2+}$ could sense $I^-$ over $S^{2-}$. Moreover, **RBP** can be successfully applied to bioimaging and detecting $Hg^{2+}$ in living cells.

## 2. Experimental

### *2.1 Material and apparatus*

All starting materials were used as received without further purification. All solvents were purified according to standard procedures unless stated otherwise. Doubly purified water used in all experiments was from Milli-Q systems. $^1$H and $^{13}$C NMR were performed on a Bruker DRX-400 spectrometer operating at 400 and 100 MHz, respectively, using TMS as an internal standard. Mass spectrometric data were collected on a PE Sciex API 3000 mass spectrometer. Elemental analyses (C, H and N) were carried out using a Perkin-Elmer 240 elemental analyser. UV-Vis absorption and fluorescence spectra were measured on a Shimadzu UV-2100 spectrophotometer

and an F-7000 spectrofluorophotometer, respectively. 2-amino-3',6'-bis(diethylamino)spiro[isoindoline-1,9'-xanthen]-3-one (**3**) was synthesized according to the literature [53].

*2.2 Synthesis*

*2.2.1 Synthesis of 6-methyl-2,2'-bipyridine (**1**)*

The title compound was synthesized using a revised procedure [54]. Methyllithium (1.3 M, 33.80 mmol) in THF (26 mL) was added dropwise to a solution of 2,2'-bipyridine (5.30 g, 34.00 mmol) in diethyl ether (100 mL) at $0^{o}C$ under $N_2$ atmosphere. The reaction mixture was stirred for 2 h, and then refluxed for 3 h. Water (10 mL) was added when the mixture cooled to room temperature. The organic layer was separated and the aqueous layer was extracted three times with ether. The combined organic layer was dried by anhydrous $Na_2SO_4$. The solvent was removed by evaporation. The resulting orange oil was oxidized with saturated $KMnO_4$/acetone (300 mL) and stirred for 1 h. The filtrate was placed in a flask and acetone was removed by evaporation. The resulting dark oil was distilled under vacuum and finally gave pure 6-methyl-2,2'-bipyridine as colourless oil (3.73 g, 63.8%). $^{1}H$ NMR (400 MHz, $CDCl_3$) $\delta$ ppm : 8.65 (s, 1H), 8.38 (d, $J$ = 8.0 Hz, 1H), 8.15 (d, $J$ = 7.9 Hz, 1H), 7.72-7.82 (m, 1H), 7.66 (d, $J$ = 7.7 Hz, 1H), 7.21-7.30 (m, 1H), 7.13 (d, $J$ = 7.7 Hz, 1H), 2.61(s, 3H). $^{13}C$ NMR (100 MHz, $CDCl_3$) $\delta$ ppm: 157.7, 156.3, 155.4, 149.0, 136.9, 136.7, 123.6, 123.2, 121.02, 117.9, 24.5. ESI-MS (m/z): calcd for $C_{11}H_{10}N_2$ $[M+H]^+$ 171.22, found 171.61.

*2.2.2 Synthesis of 2,2'-bipyridine-6-carbaldehyde (**2**)*

Compound **2** was obtained using a revised procedure [55]. A mixture of compound **1** (3.31g, 19.45 mmol) and selenium dioxide (1.27 g, 11.5 mmol) in dioxane (50 mL) containing $H_2O$ (0.21 mL) was refluxed for 3 h. After the foregoing mixture was cooled to room temperature, additional selenium dioxide (1.27 g, 11.5 mmol) and $H_2O$ (0.2 mL) was added and then the mixture was refluxed for 27 h. The hot reaction mixture was filtered and the insoluble material was washed with warm dioxane and ethyl acetate (20 mL × 3). the crude product was purified by column chromatography to give the title compound (1.28 g, 34.1%) as colourless oil. $^1$H NMR (400 MHz, $CDCl_3$) $\delta$ ppm: 10.18 (s, 1H), 8.74 (ddd, $J$ = 4.8, 1.7, 0.9 Hz, 1H), 8.65 (dd, $J$ = 7.1, 1.95 Hz, 1H), 8.56 (d, $J$ = 7.9 Hz, 1H), 7.97-8.02 (m, 2H), 7.90 (td, $J$ = 7.9, 1.8 Hz, 1H), 7.40 (ddd, $J$ = 7.1, 4.8, 1.1 Hz, 1H). $^{13}$C NMR (100 MHz, $CDCl_3$) $\delta$ ppm: 193.7, 156.6, 155.0, 152.3, 149.3, 138.0, 137.1, 125.3, 124.4, 121.5, 121.4. ESI-MS (m/z): calcd for $C_{11}H_8N_2O$ $[M+H]^+$ 185.20, found 185.15.

*2.2.3 Synthesis of 2-(2,2'-bipyridin-6-ylmethyleneamino)-3',6'-bis (diethylamino) spiro[isoindoline-1,9'-xanthen]-3-one (**RBP**)*

A mixture of Rhodamine B hydrazide (0.547 g, 1.14 mmol) and 2,2'-bipyridine-6-carbaldehyde (0.184 g, 1.00 mmol) in ethanol (20 mL) was refluxed for 6 h. The pure **RBP** as a yellow solid (0.36 g, 50.1%) was obtained by column chromatography. $^1$H NMR (400 MHz, $CDCl_3$) $\delta$ ppm: 8.84 (s, 1H), 8.31-8.60 (m, 2H), 7.70-8.03(m, 3H), 7.31-7.62 (m, 4H), 7.15 (d, $J$ = 8.3 Hz, 1H), 6.55 (t, $J$ = 8.4 Hz, 1H), 6.46 (d, $J$ = 7.7 Hz, 2H), 6.42 (d, $J$ = 7.8 Hz, 2H), 6.23-6.32 (m, 2H), 3.33 (q, $J$ = 7.0 Hz, 8H), 1.15 (t, $J$ = 6.9 Hz, 12H). $^{13}$C NMR (100 MHz, $CDCl_3$) $\delta$ ppm: 166.2,

153.8, 149.0, 148.9, 148.8, 136.9, 136.8, 132.5, 128.1, 127.9, 120.8, 120.5, 108.0, 105.9, 104.5, 97.9, 97.9, 66.2, 65.9, 44.3, 12.6. ESI-MS (m/z): calcd for $C_{39}H_{38}N_6O_2$ $[M+H]^+$ 623.3134, found 623.3174.

*2.2.4 Synthesis of 2-(benzylideneamino)-3',6'-bis(diethylamino)spiro[isoindoline-1,9'-xanthen]-3-one (**RBB**)*

**RBB** was synthesized using excess benzaldehyde in an identical procedure to **RBP** as a yellow solid (0.71 g, 65.4%). $^1$H NMR (400 MHz, $CDCl_3$) $\delta$ ppm: 8.65 (s, 1H), 7.98 (s, 1H), 7.54-7.58 (m, 2H), 7.39-7.50 (m, 2H), 7.22-7.26 (m, 3H), 7.11 (s, 1H), 6.52 (dd, $J$ = 8.8, 2.3 Hz, 2H ), 6.43 (d, $J$ = 2.3 Hz, 2H), 6.24 (dd, $J$ = 8.8, 2.3 Hz, 2H), 3.31 (q, $J$ = 7.1 Hz, 8H), 1.15 (t, $J$ = 7.1 Hz, 12H). $^{13}$C NMR (100 MHz, $CDCl_3$) $\delta$ ppm : 164.3, 153.3, 151.6, 149.0, 148.4, 135.1, 134.4, 130.8, 129.4, 128.1, 127.3, 124.4, 123.5, 108.5, 106.0, 97.8, 66.0, 44.1, 12.9. Anal. calc. for $C_{35}H_{36}N_2O_2$: C, 77.18; H, 6.66; N, 10.29; found: C, 77.24; H, 6.62; N, 10.32.

*2.3 Cell culture and confocal imaging*

MCF-7 cells were cultured in Dulbecco's Modified Eagle's Medium (DMEM, Gibco) supplemented with 10% fetal bovine serum (FBS, Gibco), and maintained in 5% $CO_2$ at 37$^o$C. 12 hours before imaging, the cells were cultured on confocal culture dishes in 1 mL of DMEM without FBS the cells were treated and incubated with 10 μM **RBP** in EtOH-$H_2O$ stock solution at 37$^o$C under 5% $CO_2$ for 30 min, and were provided with fresh medium that contained $Hg^{2+}$ (50 μM). The cells were incubated for another 10 min under the above conditions. The images were taken after the cells were rinsed three times with phosphate buffered saline (PBS).

## 3. Results and discussion

### *3.1. Synthesis*

The synthesis of compound **RBP** is shown in Scheme 2. Briefly, **2** was prepared by methyl group oxidation of 2,2'-bipyridine according to a previously reported procedure [54, 55]. Thereafter **RBP** was obtained in good yields by heating a mixture of **2** and **3** to reflux in methanol for 6 h. A reference compound 2-(benzylideneamino)-3',6'-bis(diethylamino)spiro[isoindoline-1,9'-xanthen]-3-one (**RBB**), was synthesized in good yields using the same procedure as **RBP** from benzaldehyde. **RBP** was characterized by $^{1}$H NMR, $^{13}$C NMR, and MS (SI, Figs. S1-S3). Comparison of the fluorescence emission spectra of **RBP** and **RBB** further confirmed the important role of the binding ability of bipyridyl group.

### *3.2. UV-vis and fluorescence studies*

First, the UV-Vis titration experiments of **RBP** with $Hg^{2+}$ were performed in 1:4 (v/v) EtOH/$H_2O$ solution at pH 7.0 (HEPES 20 mM). As shown in Fig. 1a, the solution of free **RBP** in EtOH/$H_2O$ (1:4, v/v) was colourless and exhibited no absorption, which is ascribed to the spirolactam form of **RBP**. Addition of $Hg^{2+}$ immediately induced a new absorption band at 568 nm which is proportional to the $Hg^{2+}$ concentration ranging from 0–33 equiv. (Inset of Fig. 1a). The maximum absorption appeared upon addition of 33 equiv. of $Hg^{2+}$. An obvious colour response of **RBP** from colourless to pink was stimulated by coordination of $Hg^{2+}$ (Fig. 1b and 1c). Such a characteristic colour change and absorption response indicates that **RBP**

can be used as a sensitive and colorimetric "naked-eye" chemosensor for $Hg^{2+}$ in environmental and biological samples.

To further examine the sensitivity, fluorescence properties of **RBP** (20 μM) with $Hg^{2+}$ were investigated in EtOH/$H_2O$ (1:4, v/v) solution (HEPES 20 mM, pH 7.0) (Fig. 2). As anticipated, a new fluorescence emission peak at 584 nm was observed upon incremental addition of $Hg^{2+}$ and finally reached the maximum in the presence of 33 equiv. of $Hg^{2+}$, an 18-fold increase over that with 1 equiv. of $Hg^{2+}$, whereas free **RBP** displayed almost no fluorescence emission upon excitation at 520 nm. This remarkable enhancement was reasonably attributed to the existing conjugated xanthene tautomer of the rhodamine moiety of **RBP**. The fluorescence quantum yield was 0.386 with Rhodamine B as a reference. In the inset of Fig. 2a, there is a good linear relationship between the emission intensity at 584 nm and the concentration of $Hg^{2+}$ ranging from 0 – 33 equiv. ($R^2$ = 0.997), which was further confirmed by the linearity of UV-Vis data. The detection limit for $Hg^{2+}$ was evaluated to be 32 nM using the equation $LOD = K*Sb/S$ (where $K$ = 3, $Sb$ is the standard deviation of the blank solution and $S$ is the slope of the calibration curve of fluorescence emission) (Fig. S4), which was much lower than the permissible limit of 0.001 mg/L (tolerable value for mercury in drinking water by the World Health Organization (WHO)) [13]. A Job's plot indicated a 1:1 binding stoichiometry with a maximum emission change observed at a mole ratio of 1:1 for **RBP** and $Hg^{2+}$ (Fig. S5). With the absorption data, the association constant $K_a$ was evaluated to be $0.95 \times 10^3$ $M^{-1}$ using the Benesi-Hildebrand equation [56]. Thereby, our supposed fluorescence method to

detect $Hg^{2+}$ provides excellent sensitivity comparable to most turn-on sensors reported in the literature (Table S1).

*3.3. pH stability studies*

To explore **RBP** applications in biological systems, the fluorescence response of **RBP,** with or without $Hg^{2+}$ at 584 nm at different pH values, was investigated (Fig. S6) in EtOH/$H_2O$ (1:4, v/v). In the absence of $Hg^{2+}$ the obvious fluorescence emission of the free **RBP** was detected only in a more acidic environment (pH < 5.0), indicating the susceptibility of the spirolactam ring. There was no any obvious change of complex **RBP**-$Hg^{2+}$ when pH was not more than 10. That is because **RBP**-$Hg^{2+}$ would decompose at strong basic conditions. This good fluorescence response of **RBP** to $Hg^{2+}$ in a wide pH range of 5 – 10 indicated that it can act as a sensitive chemosensor under physiological conditions.

*3.4. Metal Ion Competition and Anion Recognition Studies*

Competition experiments to study the selectivity of chemosensor **RBP** toward $Hg^{2+}$ over other competitive metal cations were performed and the respective fluorescence intensities are displayed in Fig. 2b. When the titration was conducted in EtOH/$H_2O$ solution (1:4, v/v, HEPES 20 mM, pH 7.0), respective addition of other competitive metal ions such as $Ag^{+}$, $Al^{3+}$, $Ba^{2+}$, $Cd^{2+}$, $Fe^{3+}$, $K^{+}$, $Li^{+}$, $Mn^{2+}$, $Na^{+}$, $Ni^{2+}$, $Pb^{2+}$, and $Zn^{2+}$ did not cause any absorption and fluorescence response of **RBP** even at a concentration of 50 equiv. of metal ions under physiological conditions. Only $Hg^{2+}$ induced a significant fluorescence enhancement; the colour change from colourless to red although $Cu^{2+}$ and $Cr^{3+}$ induced a weak fluorescence change. As shown in Fig. S7,

addition of $Hg^{2+}$ into a solution of **RBP** with other competitive metal ions together induced significant fluorescence emission. In fact, **RBP** also exhibited satisfactory selectivity toward $Hg^{2+}$ in a mixture of all competitive metal ions. These results indicate that **RBP** is highly selective chemosensor for $Hg^{2+}$ by direct visual observation in aq. ethanol solution under physical conditions.

To further verify the selectivity, the fluorescence emission of complex **RBP**-$Hg^{2+}$ was investigated with some representative anions such as $SO_4^{2-}$, $PO_4^{3-}$, $CH_3COO^-$, $CO_3^{2-}$, $NO_3^-$ $F^-$, $Cl^-$, $Br^-$, $I^-$ and $S^{2-}$ in EtOH-$H_2O$ (1:4, v/v) solution at pH 7 (HEPES 20 mM). As shown in Fig. 3a, only $I^-$ and $S^{2-}$ could dramatically quench the fluorescence intensity of the solution of **RBP** (10 μM) and $Hg^{2+}$ (30 equiv.), and induce a colour change from red to colourless. Other anions did not perturb any marked fluorescence emission of the **RBP**-$Hg^{2+}$ complex in solution except a weak fluorescence-quenching from $Br^-$. The fluorescence intensity of **RBP**-$Hg^{2+}$ decreased upon gradual addition of $I^-$ (Fig. 3b). That also indicated that $Hg^{2+}$ prefers binding with $I^-$ than **RBP**. A good linear relationship between the fluorescence change and the $I^-$ concentration was obtained during the $I^-$ range from 0-2 equiv. compared to the $Hg^{2+}$ concentration (inset of Fig. 3c). Based on $LOD = K*Sb/S$, the limit of detection (LOD) of **RBP**-$Hg^{2+}$ to $I^-$ is calculated to be 0.75 μM. The titration of $S^{2-}$ to **RBP**-$Hg^{2+}$ also was carried out and gave rise to good linearity of the fluorescence change and the $S^{2-}$ concentration with the detection limit of 0.43 μM (Fig. S8).

Response time and reversibility are fundamental parameters for most coordination-based chemosensors, and the kinetic profiles of the reaction of **RBP** and

$Hg^{2+}$, **RBP**-$Hg^{2+}$ and $I^-$, and **RBP**-$Hg^{2+}$ and $S^-$, respectively, at room temperature was examined. The fluorescence emission reached maximum within 70 minutes (Fig. S9). Surprisingly the binding of $I^-$ to $Hg^{2+}$ from the **RBP**-$Hg^{2+}$ complex was over in ca. 10 seconds and the fluorescence emission was unchanged over the subsequent 120 s (Fig. 3d). However, the reaction between $S^{2-}$ and $Hg^{2+}$ from **RBP**-$Hg^{2+}$ almost finished in almost 30 minutes, which is much longer than that of $I^-$ (Fig. S10). Therefore, **RBP**-$Hg^{2+}$ still can rapidly sense $I^-$ in few seconds even in the presence of $S^{2-}$ interference. The recyclability experiments of **RBP** upon the addition of $Hg^{2+}$ and subsequent $I^-/S^{2-}$ were carried out and confirmed the high stability of **RBP** in EtOH/$H_2O$ solution although a slightly attenuation was found, which fully support the reversible spirolactam ring-opening mechanism of rhodamine derivatives (Fig. S11). These results indicated that **RBP** can be a selective and sensitive $Hg^{2+}$ chemosensor and its resultant complex can fast detect $I^-$.

*3.5. The proposed sensing mechanism*

Up to now turn-on fluorescent chemosensors are still preferable due to high selectivity, sensitivity and ease of observation compared to turn-off ones. The fluorescence enhancement of **RBP** toward $Hg^{2+}$ is supposed to arise from the spiro ring-opening mechanism rather than an ion-catalysed hydrolysis reaction. So a plausible response mechanism of **RBP** to $Hg^{2+}$ is shown in Scheme S1. Based on this, **RBP** was rationally designed containing the rhodamine B platform as the potential strong fluorophore, and a bipyridyl fragment as a specific binding receptor of $Hg^{2+}$. The bipyridyl fragment binding with $Hg^{2+}$ induced opening of the

spirolactam ring of rhodamine moiety, which caused the enhancement of fluorescence and colour changes. Addition of $I^-$ led to the regeneration of the no-fluorescence spirolactam ring of rhodamine moiety of **RBP** because of the strong binding ability between $I^-$ and $Hg^{2+}$ which causes the formation of $HgI_2$. Although compared with $I^-$, $S^{2-}$ binds $Hg^{2+}$ much more slowly, the reaction still can finish about 30 minutes. A second addition of $Hg^{2+}$ also recovered the fluorescence emission. Thus, the reversibility evidently ruled out the possibility of hydrolysis mentioned in the literature [57]. In order to confirm the importance of the bipyridyl fragment, **RBB** was synthesized and studied by fluorescence emission spectra in EtOH/$H_2O$ (1:4, v/v). As shown in Fig. S12, **RBB** did not generate any fluorescence emission even with excess addition of 100 equiv. of $Hg^{2+}$, which confirmed the crucial role of the bipyridyl group of **RBP**. Job's plot also ascertained a 1:1 stoichiometry of **RBP** and $Hg^{2+}$.

*3.6. Cytotoxicity and application of **RBP** in living cells*

The excellent absorbance and fluorescence spectroscopic properties of **RBP** inspired us to carry out the $Hg^{2+}$ bioimaging studies using MCF-7 cells with a confocal microscope Zeiss LSM710 (Fig. 4). MCF-7 cells were cultured with **RBP** (10 μM) in DMEM for 30 min at 37°C and washed with PBS buffer. No intracellular fluorescence was detected (Figs. 4a and 4b), indicating that the probe **RBP** maintained its spirolactam form in cells. When the MCF-7 cells pre-incubated with **RBP** and further treated with 50 μM $Hg^{2+}$ for 10 min, an intense red fluorescence was observed (Figs. 4c and 4d). This phenomenon illustrated **RBP** was cell permeable, and could sense $Hg^{2+}$ in living cells. We further performed a conventional MTT assay

to examine the cytotoxicity of **RBP** on MCF-7 cells, in which no cytotoxicity was observed, even at **RBP** concentrations up to 100 μM. These results indicated that probe **RBP** could viably sense $Hg^{2+}$ both in vitro and in vivo cells.

## 4. Conclusions

In conclusion, we have developed a colorimetric and fluorescent chemosensor **RBP** for $Hg^{2+}$ detection with high selectivity and sensitivity under physiological conditions. Moreover, the ensemble **RBP**-$Hg^{2+}$ can be an excellent sensory system for fast detection $I^-$ over $S^{2-}$ with reversibility, indicating that the metal-based complex is a promising tool to selectively and sensitively detect anions. The confocal fluorescence image confirmed that **RBP** owes high cell permeability and low toxicity for sensing $Hg^{2+}$ in vivo cells. We believe that the proposed strategy can be applied to construct other multifunctional fluorescent probes owing wide potential applications in environmental and biological analysis, or in vivo cells.

**Acknowledgements**

We thank the national Natural Science Foundation of china (Grant No. 21101074, 21222502, 21575032), Shandong Provincial Natural Science Foundation of China (Grant No. ZR2013BQ009), and the Doctor's Foundation of University of Jinan (Grant No. XBS1320) for funding. Dr. Srinivas Abbina from Center for Blood Research, Department of Pathology and Laboratory Medicine, University of British Columbia, Canada is kindly acknowledged for his constructive comments and suggestions to improve the manuscript significantly.

## References

[1] Hussain S, De S, Iyer PK. Thiazole-containing conjugated polymer as a visual and fluorometric sensor for Iodide and mercury. ACS Appl Mater Interfaces 2013;5:2234-40.

[2] Fitzgerald WF, Lamborg CH, Hammerschmidt CR. Marine biogeochemical cycling of mercury. Chem Rev 2007;107:641-62.

[3] Li Y, Zhang X, Zhu B, Xue J, Zhu Z, Tan W. A simple but highly sensitive and selective colorimetric and fluorescent probe for $Cu^{2+}$ in aqueous media. Analyst 2011;136:1124-8.

[4] Wang H, Xue L, Jiang H. Ratiometric fluorescent sensor for silver ion and its resultant complex for iodide anion in aqueous solution. Org Lett 2011;13:3844-7.

[5] Nolan EM, Lippard SJ. Tools and tactics for the optical detection of mercuric ion. Chem Rev 2008;108:3443-80.

[6] Zalups RK. Molecular interactions with mercury in the kidney. Pharmacol Rev 2000;52:113-43.

[7] Renzoni A, Zino F, Franchi E. Mercury levels along the food chain and Risk for exposed populations. Environ Res 1998;77:68-72.

[8] Hoyle I, Handy RD. Dose-dependent inorganic mercury absorption by isolated perfused intestine of rainbow trout, Oncorhynchus mykiss, involves both amiloride-sensitive and energy-dependent pathways. Aquat Toxicol 2005;72:147-59.

[9] Zhang X, Xiao Y, Qian X. A ratiometric fluorescent probe based on FRET for imaging $Hg^{2+}$ ions in living cells. Angew Chem Int Ed 2008;47:8025-9.

[10] Cao Q-Y, Han Y-M, Wang H-M, Xie Y. A new pyrenyl-appended triazole for fluorescent recognition of $Hg^{2+}$ ion in aqueous solution. Dyes and Pigments 2013;26:798-802.

[11] Harada M. Minamata disease: methylmercury poisoning in Japan caused by environmental pollution. Crit Rev Toxicol 1995;25:1-24.

[12] Onyido I, Norris AR, Buncel E. Biomolecule-mercury interactions: modalities of DNA base-mercury binding mechanisms. Remediation strategies. Chem Rev 2004;104:5911-29.

[13] Lisha KP, Pradeep T. Toward a practicl solution for removing inorganic mercury from drinking water using gold nanoparticles. Gold Bull 2009;42:144-52.

[14] Martínez-Máñez R, Sancenón F. Fluorogenic and chromogenic chemosensors and reagents for anions. Chem Rev 2003;103:4419-76.

[15] Mahapatra AK, Roy J, Sahoo P, Mukhopadhyay SK, Chattopadhyay A. Carbazole–thiosemicarbazone–Hg(II) ensemble-based colorimetric and fluorescence turn-on toward iodide in aqueous media and its application in live cell imaging. Org Biomol Chem 2012;10:2231-6.

[16] Qandil AM. Prodrugs of nonsteroidal anti-inflammatory drugs(NSAIDs), more than meets the eye: A critical review Int J Mol Sci 2012;13:17244-74.

[17] Haldimann M, Zimmerli B, Als C, Gerber H. Direct determination of urinary iodine by inductively coupled plasma mass spectrometry using isotope dilution with iodine-129. Clin Chem 1998;44:817-24.

[18] Dwight SJ, Gaylord BS, Hong JW, Bazan GC. Perturbation of fluorescence by nonspecific interactions between anionic poly(phenylenevinylene)s and proteins: Implications for biosensors. J Am Chem Soc 2004;126:16850-9.

[19] Eto K, Asada T, Arima K, Makifuchi T, Kimura H. Brain hydrogen sulfide is severely decreased in Alzheimer's disease. Biochem Biophys Res Commun 2002;293:1485-8.

[20] Kamoun P, Belardinelli MC, Chabli A, Lallouchi K, Chadefaux-Vekemans B. Endogenous hydrogen sulfide overproduction in Down syndrome. Am J Med Genet 2003;116A:310-1.

[21] Yang W, Yang G, Jia X, Wu L, Wang R. Activation of $K_{ATP}$ channels by $H_2S$ in rat

insulin-secreting cells and the underlying mechanisms. J Physiol 2005;569:519-31.

[22] Łowicka E, Bełtowski J. Hydrogen sulfide ($H_2S$)-the third gas of interest for pharmacologists. Pharmacol Rep 2007;59:4-24.

[23] Yang X, Wang L, Xu H, Zhao M. A fluorescein-based fluorogenic and chromogenic chemodosimeter for the sensitive detection of sulfide anion in aqueous solution. Anal Chim Acta 2009;631:91-5.

[24] Zhou G, Wang H, Ma Y, Chen X. An NBD fluorophore-based colorimetric and fluorescent chemosensor for hydrogen sulfide and its application for bioimaging. Tetrahedron 2013;69:867-70.

[25] Chen X, Zhou G, Peng X, Yoon J. Fluorescent and colorimetric probes for detection of thiols. Chem Soc Rev 2010;39:2120-35.

[26] Fan J, Hu M, Zhan P, Peng X. Energy transfer cassettes based on organic fluorophores: construction and applications in ratiometric sensing. Chem Soc Rev 2013;42:29-43.

[27] Martínez-Máñez R, Sancenón F. Fluorogenic and chromogenic chemosensors and reagents for anions. Chem Rev 2003;103(11):4419-76.

[28] Li X, Sun L, Ding T. Multiplexed sensing of mercury(II) and silver(I) ions: a new class of DNA electrochemiluminescent-molecular logic gates. Biosens Bioelectron 2011;26:3570-6.

[29] Srivastava P, Razi SS, Ali R, Gupta RC, Yadav SS, Narayan G, et al. Selective naked-eye detection of $Hg^{2+}$ through an efficient Turn-on photoinduced electron transfer fluorescent probe and its real applications. Anal Chem 2014;86:8693-9.

[30] Wang M, Wen J, Qin ZH, Wang HM. A new coumarin-rhodamine FRET system as an efficient ratiometric fluorescent probe for $Hg^{2+}$ in aqueous solution and in living cells. Dyes Pigm 2015;120:208-12.

[31] Dai BN, Cao QY, Wang L, Wang ZC, Yang ZY. A new naphthalene-containing triazolophane for fluorescence sensing of mercury(II) ion. Inorg chim Acta 2014;423:163-7.

[32] Xiao HD, Li JH, Wu KT, Yin G, Quan YW, Wang RY. A turn-on BODIPY-based fluorescent probe for Hg(II) and its biological applications. Sens Actuators B 2015;213:343-50.

[33] Wu B, Xu L, Wang SF, Wang Y, Zhang WA. A PEGylated colorimetric and turn-on fluorescent sensor based on BODIPY for Hg(II) detection in water. Polym Chem 2015;6:4279-89.

[34] Yoon S, Albers AE, Wong AP, Chang CJ. Screening mercury levels in fish with a selective fluorescent chemosensor. J Am Chem Soc 2005;127:16030-1.

[35] He X, Zhang J, Liu X, Dong L, Li D, Qiu H, et al. A novel BODIPY-based colorimetric and fluorometric dual-mode chemosensor for $Hg^{2+}$ and $Cu^{2+}$. Sens Actuators B 2014;192:29-35.

[36] Kaur A, Raj T, Kaur S, Singh N, Kaur N. Fluorescent organic nanoparticles of dihydropyrimidone derivatives for selective recognition of iodide using a displacement assay: application of the sensors in water and biological fluids. Org Biomol Chem 2015;13:1204-12.

[37] Nabavi S, Alizadeh N. A highly sensitive and selective turn-on fluorescence sensor for iodide detection based on newly synthesized oligopyrrole derivative and application to real samples. Sens Actuators B 2014;200:76-82.

[38] Corma A, Galletero MS, García H, Palomares E, Rey F. Pyrene covalently anchored on a large external surface area zeolite as a selective heterogeneous sensor for iodide. Chem Commun 2002:1100-1.

[39] Zheng KB, Lin WY, Tan L, Cheng D. A two-photon fluorescent probe with a large turn-on signal for imaging hydrogen sulfide in living tissues. Anal Chim Acta 2015;853:548-54.

[40] Zhang CY, Wei L, Wei C, Zhang J, Wang RY, Xi Z, et al. A FRET–ICT dual-quenching fluorescent

probe with large off–on response for $H_2S$: synthesis, spectra and bioimaging. Chem Commun 2015;51:7505-8.

[41] Zhang C, Peng B, Chen W, Shuang S, Xian M, Dong C. A ratiometric fluorescent probe for hydrogen sulfide based on the nucleophilic substitution-cyclization of diselenides. Dyes Pigm 2015;121:299-304.

[42] Wu X, Chen J, Zhao JX. A reversible fluorescent logic gate for sensing mercury and iodide ions based on a molecular beacon. Analyst 2013;138:5281-7.

[43] Meng QT, Shi Y, Wang CP, Jia HM, Gao X, Zhang R, et al. NBD-based fluorescent chemosensor for the selective quantification of copper and sulfide in an aqueous solution and living cells. Org Biomol Chem 2015;13:2918-26.

[44] Huang K, Yu L, Xu P, Zhang X, Zeng W. A novel FRET-based ratiometric fluorescent probe for highly sensitive detection of hydrogen sulfide. RSC Adv 2015;5:17797-801.

[45] Wu DY, Huang W, Duan CY, Lin ZH, Meng QJ. Highly sensitive fluorescent probe for selective detection of $Hg^{2+}$ in DMF aqueous media. Inorg Chem 2007;46:1538-40.

[46] Zhao Y, Zhang XB, Han ZX, Qian L, Li CY, Jian LX, et al. Highly Sensitive and Selective colorimetric and off-on fluorescent chemosensor for $Cu^{2+}$ in aqueous solution and living cells. Anal Chem 2009;81:7022-30.

[47] Mahapatra AK, Manna SK, Mukhopadhyay SK, Banik A. First rhodamine-based 'off-on' chemosensor with high selectivity and sensitivity for $Zr^{4+}$ and its imaging in living cell. Sens Actuators B 2013;183:350-5.

[48] O'Neil EJ, Smith BD. Anion recognition using dimetallic coordination complexes. Coord Chem Rev 2006;250:3068-80.

[49] Wei L, Zhu Z, Li Y, Yi L, Xi Z. A highly selective and fast-response fluorescent probe for visualization of enzymatic $H_2S$ production *in vitro* and in living cells. Chem Commun 2015;51:10463-6.

[50] Chung SY, Nam SW, Lim J, Park S, Yoon J. A highly selective cyanide sensing in watervia fluorescence change and its application to in vivo imaging. Chem Commun 2009:2866-8.

[51] Rochat S, Severin K. A simple fluorescence assay for the detection of fluoride in water at neutral pH. Chem Commun 2011;47:4391-3.

[52] Yang WG, Yang SH, Guo QR, Zhang T, Wu KY, Hu YH. Phenothiazine-aminothiourea-Hg(II) ensemble-based fluorescence turn-on toward iodide in aqueous media and imaging application in live cells. Sens Actuators B 2015;213:404-8.

[53] Xiang Y, Tong A, Jin P, Ju Y. New fluorescent rhodamine hydrazone chemosensor for Cu(II) with high selectivity and sensitivity. Org Lett 2006;8:2863-6.

[54] Lu ZL, Ladrak T, Roubeau O, van Der Toorn J, Teat SJ, Massera C, et al. Selective, catalytic aerobic oxidation of alcohols using $CuBr_2$ and bifunctional triazine-based ligands containing both a bipyridine and a TEMPO group. Dalton Trans 2009:3559-70.

[55] Heirtzle FR, Neuburger M, Zehnder M, Constable EC. Preparation and characterization of oligo-(2,2'-bipyridyl)pyrazines. Eur J Org Chem 1997;1997:297-301.

[56] Benesi HA, Hildebrand JH. A spectrophotometric investigation of the interaction of iodine with aromatic hydrocarbons. J Am Chem Soc 1949;71:2703-7.

[57] Gong Y-J, Zhang X-B, Chen Z, Yuan Y, Jin Z, Mei L, et al. An efficient rhodamine thiospirolactam-based fluorescenct probe for detection of $Hg^{2+}$ in aqueous samples. Analyst 2012;137:932-8.

**Scheme and Figure Captions**

**Scheme 1**. The structures of formerly reported probes.

**Scheme 2**. Structures and the syntheses of the RBP and RBB.

**Fig. 1**. (a) UV-Vis absorption spectra of probe **RBP** (10 μM) upon addition of $Hg^{2+}$ (0 - 36 equiv.) in EtOH/$H_2O$ (1:4, v/v) solution (HEPES 20 mM, pH 7.0). Inset: Calibration plot of absorption and concentration of $Hg^{2+}$. (b) Colour change of **RBP** upon interaction with different metal ions ($Hg^{2+}$, $Ag^{+}$, $Al^{3+}$, $Ba^{2+}$, $Ca^{2+}$, $Cd^{2+}$, $Fe^{3+}$, $K^{+}$, $Li^{+}$, $Mg^{2+}$, $Mn^{2+}$, $Na^{+}$, $Ni^{2+}$, $Pb^{2+}$, $Zn^{2+}$). (c) Colour change of **RBP** upon addition of $Hg^{2+}$ (0 - 36 equiv.).

**Fig. 2**. (a) Fluorescence spectra of **RBP** (10 μM) upon addition of $Hg^{2+}$ (0 - 36 equiv.) in EtOH-$H_2O$ (1:4, v/v) solution (HEPES 20 mM, pH 7.0). Inset: Calibration plot of fluorescence intensity and concentration of **RBP**. (b) Fluorescence intensity at 584 nm of **RBP** (10 μM) upon addition of 15 equiv. of various metal ions (Red bars: **RBP** with other metals, green bars: **RBP** with other metals and $Hg^{2+}$) in EtOH/$H_2O$ (1:4, v/v) solution (HEPES 20 mM, pH 7.0).1, blank; 2, $Ag^{+}$; 3, $Al^{3+}$; 4, $Ba^{2+}$; 5, $Ca^{2+}$; 6, $Cd^{2+}$; 7, $Cr^{3+}$; 8, $Cu^{2+}$; 9, $Fe^{3+}$; 10, $K^{+}$; 11, $Li^{+}$; 12, $Mg^{2+}$; 13, $Mn^{2+}$; 14, $Na^{+}$; 15, $Ni^{2+}$;16, $Pb^{2+}$; 17, $Zn^{2+}$.

**Fig. 3**. (a) Fluorescence spectra of **RBP**-$Hg^{2+}$ (10 μM) upon addition of various anions (60 equiv.) in EtOH-$H_2O$ (1:4, v/v) solution (HEPES 20 mM, pH 7.0). (b) Fluorescence intensity of **RBP**-$Hg^{2+}$ (10 μM) upon addition of $I^{-}$ (0-2 equiv. of $Hg^{2+}$) in EtOH-$H_2O$ (1:4, v/v) solution (HEPES 20 mM, pH 7.0). (c) Calibration plot of fluorescence intensity and concentration of $I^{-}$. (d) Fluorescence intensity of

**RBP**-$Hg^{2+}$ (10 μM) upon adding 2 equiv. of $I^-$ in EtOH/$H_2O$ (1:4, v/v) solution (HEPES 20 mM, pH 7.0) as a function of the time.

**Fig. 4.** Images of MCF-7 cells treated with **RBP** (20 μM) in the absence or presence of $Hg^{2+}$ (100 μM). (a) Confocal fluorescence image of MCF-7 cells with **RBP**. (b) Bright field image of (a). (c) Confocal fluorescent image of MCF-7 cell with $Hg^{2+}$ and **RBP**. (d) Bright field image of (c). Excitation wavelengths of **RBP** and **RBP**-$Hg^{2+}$ are 543 nm. The scale bar of all figures is 20 μm.

**Scheme 1.** The structures of formerly reported probes.

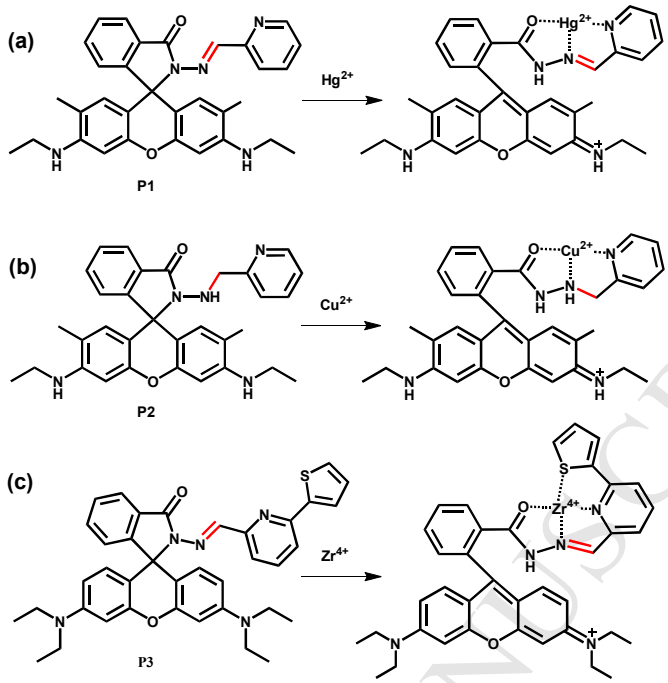


**Scheme 2**. Structures and the syntheses of the RBP and RBB.

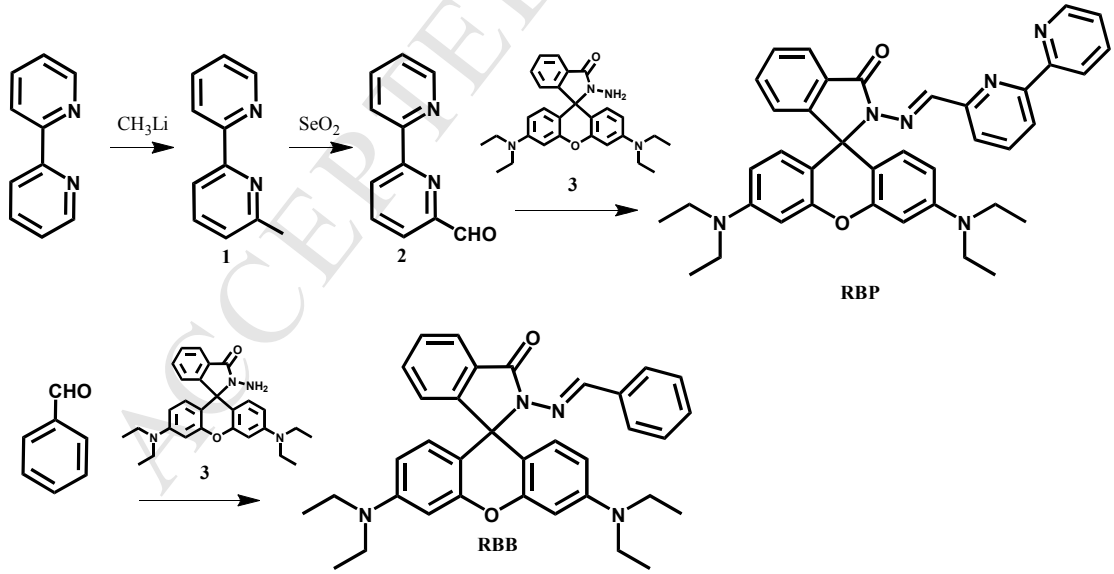

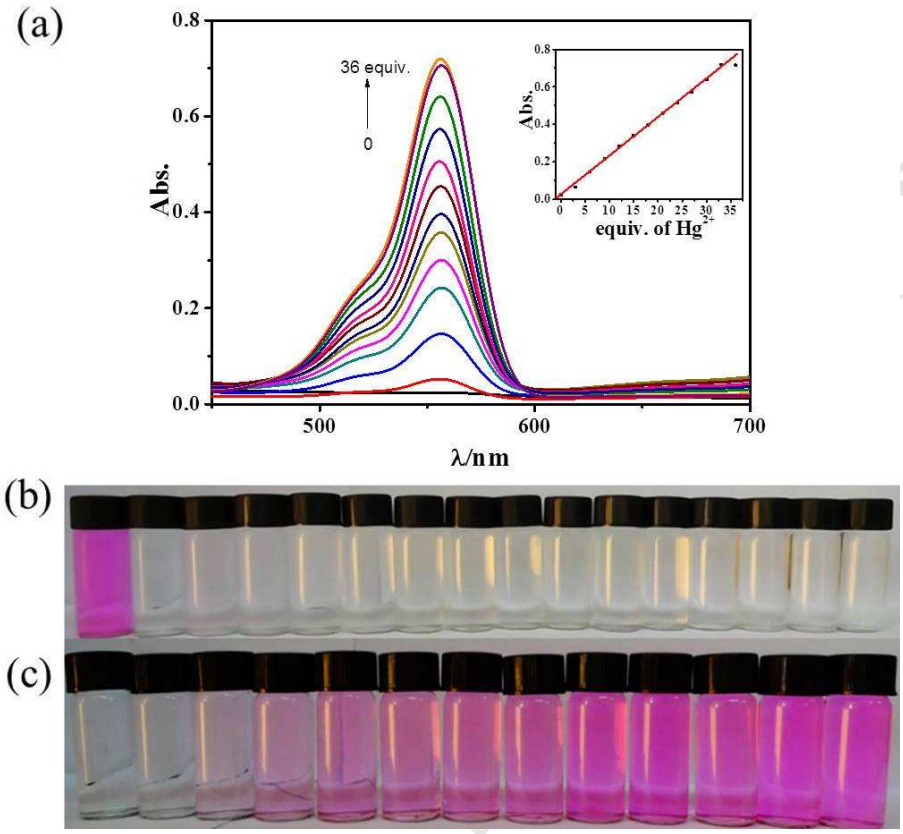


**Fig. 1**. (a) UV-Vis absorption spectra of probe **RBP** (10 μM) upon addition of $Hg^{2+}$ (0 - 36 equiv.) in EtOH/$H_2O$ (1:4, v/v) solution (HEPES 20 mM, pH 7.0). Inset: Calibration plot of absorption and concentration of $Hg^{2+}$. (b) Colour change of **RBP** upon interaction with different metal ions ($Hg^{2+}$, $Ag^{+}$, $Al^{3+}$, $Ba^{2+}$, $Ca^{2+}$, $Cd^{2+}$, $Fe^{3+}$, $K^{+}$, $Li^{+}$, $Mg^{2+}$, $Mn^{2+}$, $Na^{+}$, $Ni^{2+}$, $Pb^{2+}$, $Zn^{2+}$). (c) Colour change of **RBP** upon addition of $Hg^{2+}$ (0 - 36 equiv.).

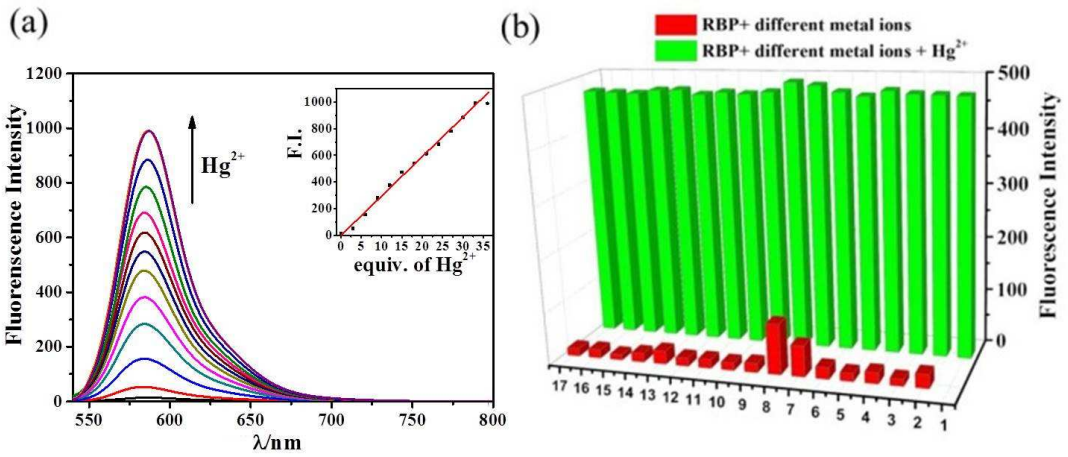


**Fig. 2**. (a) Fluorescence spectra of **RBP** (10 μM) upon addition of $Hg^{2+}$ (0 - 36 equiv.) in EtOH-$H_2O$ (1:4, v/v) solution (HEPES 20 mM, pH 7.0). Inset: Calibration plot of fluorescence intensity and concentration of **RBP**. (b) Fluorescence intensity at 584 nm of **RBP** (10 μM) upon addition of 15 equiv. of various metal ions (Red bars: **RBP** with other metals, green bars: **RBP** with other metals and $Hg^{2+}$) in EtOH/$H_2O$ (1:4, v/v) solution (HEPES 20 mM, pH 7.0).1, blank; 2, $Ag^{+}$; 3, $Al^{3+}$; 4, $Ba^{2+}$; 5, $Ca^{2+}$; 6, $Cd^{2+}$; 7, $Cr^{3+}$; 8, $Cu^{2+}$; 9, $Fe^{3+}$; 10, $K^{+}$; 11, $Li^{+}$; 12, $Mg^{2+}$; 13, $Mn^{2+}$; 14, $Na^{+}$; 15, $Ni^{2+}$;16, $Pb^{2+}$; 17, $Zn^{2+}$.

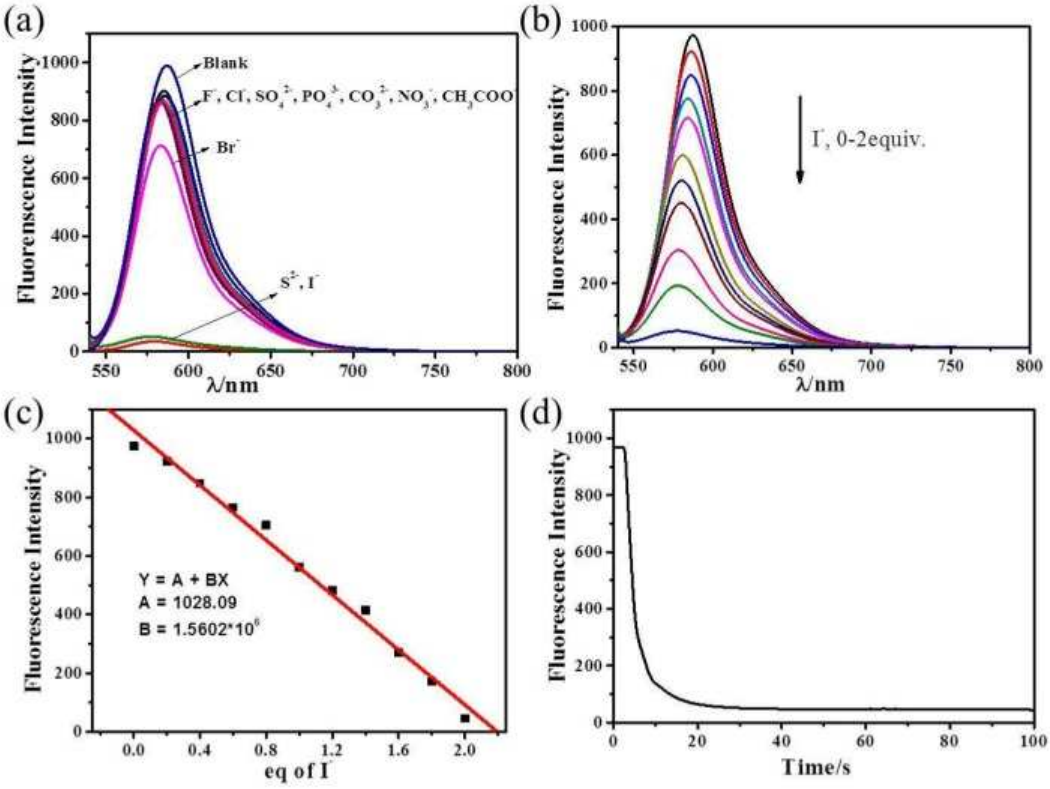


**Fig. 3**. (a) Fluorescence spectra of **RBP**-$Hg^{2+}$ (10 μM) upon addition of various anions (60 equiv.) in EtOH-$H_2O$ (1:4, v/v) solution (HEPES 20 mM, pH 7.0). (b) Fluorescence intensity of **RBP**-$Hg^{2+}$ (10 μM) upon addition of $I^-$ (0-2 equiv. of $Hg^{2+}$) in EtOH-$H_2O$ (1:4, v/v) solution (HEPES 20 mM, pH 7.0). (c) Calibration plot of fluorescence intensity and concentration of $I^-$. (d) Fluorescence intensity of **RBP**-$Hg^{2+}$ (10 μM) upon adding 2 equiv. of $I^-$ in EtOH/$H_2O$ (1:4, v/v) solution (HEPES 20 mM, pH 7.0) as a function of the time.

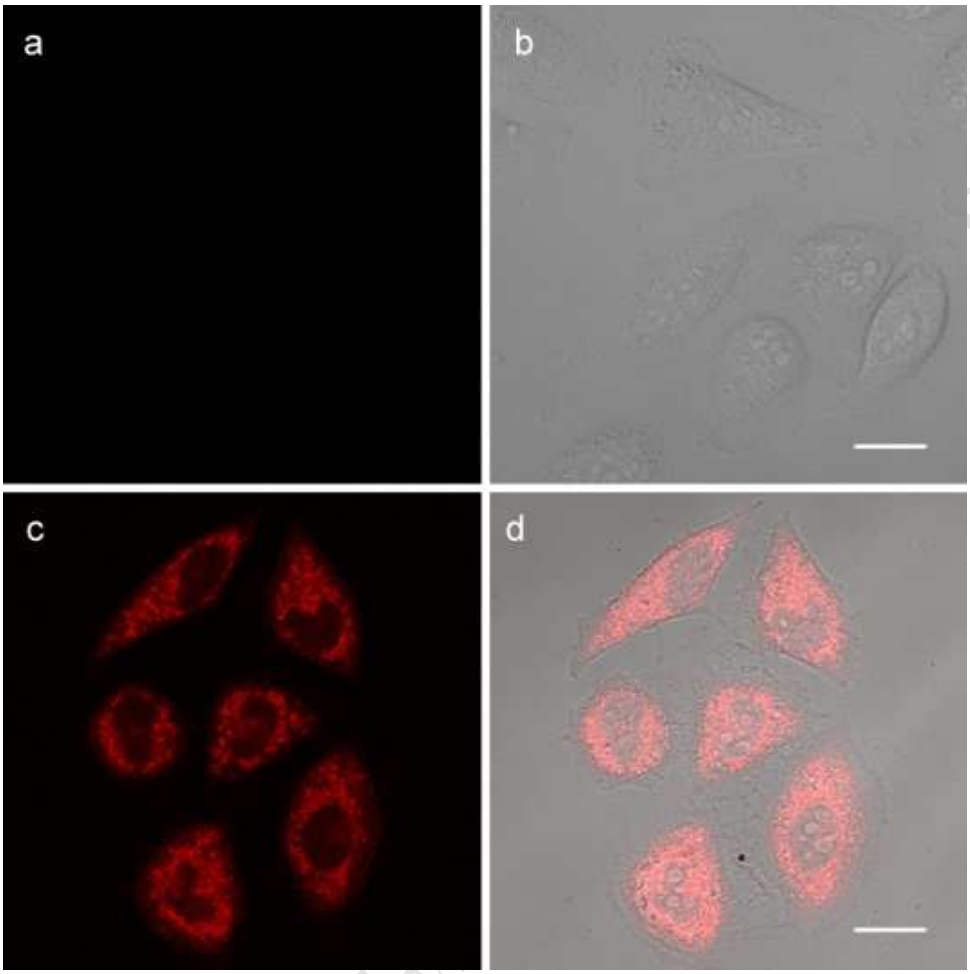


**Fig. 4.** Images of MCF-7 cells treated with **RBP** (20 μM) in the absence or presence of $Hg^{2+}$ (100 μM). (a) Confocal fluorescence image of MCF-7 cells with **RBP**. (b) Bright field image of (a). (c) Confocal fluorescent image of MCF-7 cell with $Hg^{2+}$ and **RBP**. (d) Bright field image of (c). Excitation wavelengths of **RBP** and **RBP**-$Hg^{2+}$ are 543 nm. The scale bar of all figures is 20 μm.

A colorimetric multifunctional sensor **RBP** was synthesized.

The sensor exhibited a selective fluorescence enhancement response to $Hg^{2+}$.

The resultant sensor-$Hg^{2+}$ complex rapidly detected $I^{-}$ over $S^{2-}$.

The sensor was successfully used to selectively detect $Hg^{2+}$ in living cells.